

David R. Cooper, Tomasz Boczek,† Katarzyna Grelewska,‡ Malgorzata Pinkowska,‡ Malgorzata Sikorska,§ Michal Zawadzki¶ and Zygmunt Derewenda*

Department of Molecular Physiology and Biological Physics and the Integrated Center for Structure-Function Innovation, University of Virginia, Charlottesville, Virginia 22908-0736, USA

† On leave from the Technical University of Lodz, Poland.

§ On leave from the University of Wroclaw, Wroclaw, Poland.

¶ On leave from the Jagiellonian University, Krakow, Poland.

Correspondence e-mail: zsd4n@virginia.edu

Protein crystallization by surface entropy reduction: optimization of the SER strategy

A strategy of rationally engineering protein surfaces with the aim of obtaining mutants that are distinctly more susceptible to crystallization than the wild-type protein has previously been suggested. The strategy relies on replacing small clusters of two to three surface residues characterized by high conformational entropy with alanines. This surface entropy reduction (or SER) method has proven to be an effective salvage pathway for proteins that are difficult to crystallize. Here, a systematic comparison of the efficacy of using Ala, His, Ser, Thr and Tyr to replace high-entropy residues is reported. A total of 40 mutants were generated and screened using two different procedures. The results reaffirm that alanine is a particularly good choice for a replacement residue and identify tyrosines and threonines as additional candidates that have considerable potential to mediate crystal contacts. The propensity of these mutants to form crystals in alternative screens in which the normal crystallization reservoir solutions were replaced with 1.5 M NaCl was also examined. The results were impressive: more than half of the mutants yielded a larger number of crystals with salt as the reservoir solution. This method greatly increased the variety of conditions that yielded crystals. Taken together, these results suggest a powerful crystallization strategy that combines surface engineering with efficient screening using standard and alternate reservoir solutions.

Received 22 January 2007

Accepted 8 March 2007

PDB References: RhoGDI CY mutant (K135Y,K138Y,K141Y), 2bxw, r2bxwsf; RhoGDI CH mutant (K135H,K138H,K141H), 2jhs, r2jhssf; RhoGDI CT mutant (K135T,K138T,K141T), 2jht, r2jhtsf; RhoGDI EA1 mutant (E154A,E155A), 2jhu, r2jhusf; RhoGDI EA2 mutant (E154A,E155A), 2jhv, r2jhvsf; RhoGDI FA mutant (E155A, E157A), 2jhw, r2jhwsf; RhoGDI FH1 mutant (E155H, E157H), 2jhx, r2jhxsf; RhoGDI FH2 mutant (E155H, E157H), 2jhy, r2jhysf; RhoGDI FS mutant (E155S, E157S), 2jhz, r2jhzsf; RhoGDI DY mutant (K138Y, K141Y), 2ji0, r2ji0sf.

1. Introduction

Preparation of X-ray quality crystals for structural analyses continues to be a limiting step for small research groups, high-throughput structural genomics centers and industrial laboratories. This is despite the fact that automation of the screening process has dramatically increased its speed while simultaneously decreasing the amount of protein necessary for each drop, allowing a larger number of conditions to be screened for every protein (Stevens, 2000). It follows that merely increasing the scope of the screens in crystallization trials does not address the problem of those macromolecules or their complexes that are simply recalcitrant to nucleation and/or crystal growth. The increased throughput resulting from automation of the screening process has revealed that the law of diminishing returns applies to protein crystallization. As a result, the success rates reported for crystallization in high-throughput laboratories vary from only few percent for eukaryotic proteins to ~25–30% for prokaryotic proteins, even when the protein sequences do not suggest any potential difficulties for crystallization.

It is widely recognized that certain proteins have an inherent tendency to crystallize and will do so in a wide range

of conditions, while others are less likely to form crystals even when thousands of conditions are screened (Dale *et al.*, 2003). In our previous studies, we argued that this difference can be attributed to distinct surface properties and to specific amino acids which impede the nucleation/crystallization process (Longenecker, Garrard *et al.*, 2001; Mateja *et al.*, 2002). We suggested that residues with high intrinsic conformational entropy such as lysines, glutamines and glutamates reduce the ability of proteins to crystallize by increasing the entropic barrier that must be overcome to order and bury these residues at the point of crystal contacts. Others have also argued that this is a general evolutionary mechanism by which proteins maintain solubility in the cell and avoid serendipitous protein–protein interactions (Doye, 2004). To overcome the problem, we proposed that clusters of such amino acids, typically two or three close together in sequence and in space, be replaced with low-entropy residues (*e.g.* alanines) to generate patches that would show a higher propensity to mediate crystal contacts (Longenecker, Garrard *et al.*, 2001; Mateja *et al.*, 2002). We also showed that single-site mutants are not as effective, although they often significantly affect crystallization kinetics. This approach, referred to as surface-entropy reduction (SER), has been shown to be effective in a model system and was subsequently used to crystallize a number of novel proteins both in our laboratory (Longenecker, Lewis *et al.*, 2001; Janda, Devedjiev, Cooper *et al.*, 2004; Devedjiev *et al.*, 2004; Janda, Devedjiev, Derewenda *et al.*, 2004; Bielnicki *et al.*, 2006) as well as in a number of other groups (Prag *et al.*, 2003; Nadella *et al.*, 2005; Munshi *et al.*, 2003; Grueninger & Schulz, 2006; Hu & Hubbard, 2006).

Given the success of this method, we wondered whether we could enhance its efficacy further by (i) optimizing the choice

of residues selected to replace the high-entropy amino acids, (ii) optimizing the screening process to exploit the full potential of the crystallizable mutants and (iii) automating the process of the selection of suitable clusters for mutagenesis based on amino-acid sequence alone. The third objective has been achieved through a new SER-prediction (SERp) server, a freely accessible web-based interactive tool available to the general public (<http://nihserver.mbi.ucla.edu/SER>) and described in a separate publication (Goldschmidt *et al.*, in preparation). Here, we address the former two issues.

Alanine, an amino acid with no side-chain conformational entropy, was originally chosen to test the basic premise of the approach (Longenecker, Garrard *et al.*, 2001). While it has been shown by us and others to be effective, we also noted that some RhoGDI mutants with alanine substitutions show compromised solubility (Longenecker, Garrard *et al.*, 2001). We therefore asked whether small but more polar residues such as Ser and Thr might be equally effective for enhancement of crystallization without decreasing solubility. We also wondered whether other residues, such as His and Tyr, which have limited side-chain conformational freedom and are found to be ubiquitous at protein–protein interfaces (Conte *et al.*, 1999), might mediate crystal contacts.

To address these questions, we again used the globular domain of human RhoGDI as a model system. This relatively small and easily produced and purified protein contains 10% Lys and 8% Glu and is recalcitrant to crystallization in the wild-type form (Longenecker, Garrard *et al.*, 2001; Sheffield *et al.*, 1999). Its rich ‘entropic shield’ makes it a superb model system, which is the reason why we used it in previous studies (Longenecker, Garrard *et al.*, 2001; Mateja *et al.*, 2002; Czepas *et al.*, 2004). We selected a number of sites suitable for surface

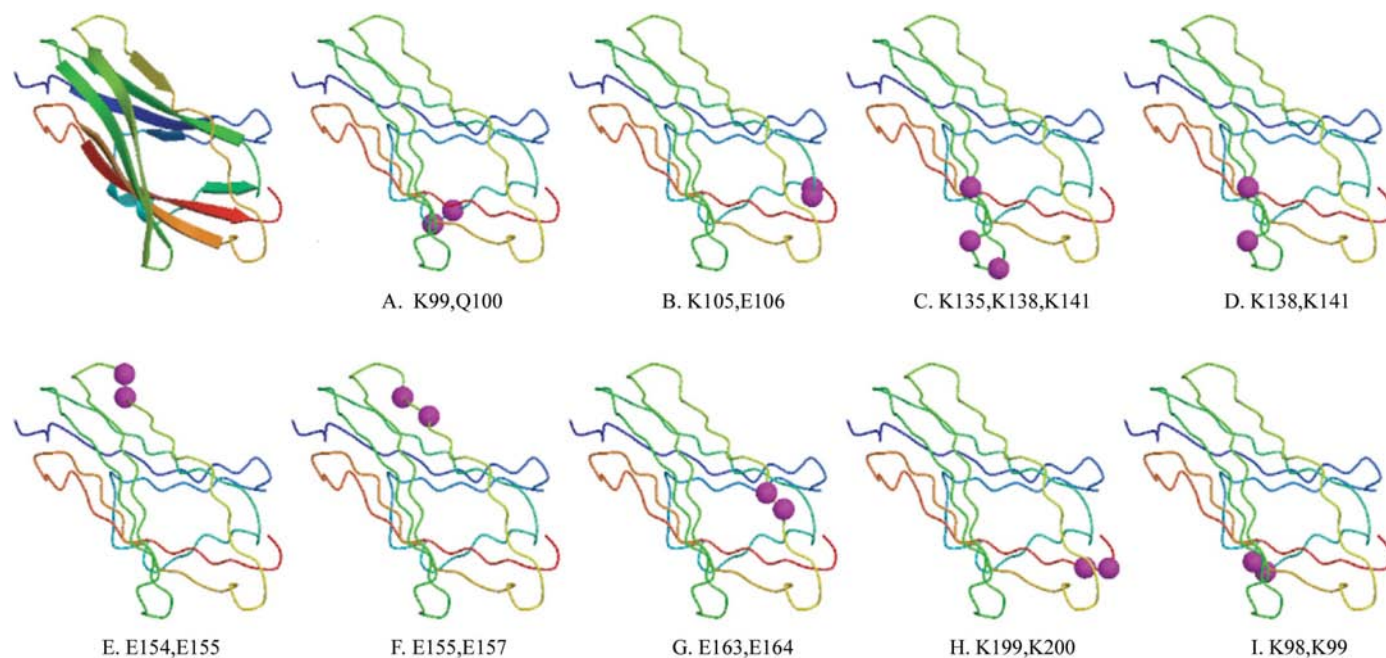


Figure 1

The distribution of the mutations used in this study. The mutation clusters were designated by a single letter A–I. The mutations corresponding to each cluster are shown as magenta spheres on the ribbon diagram. A cartoon representation of RhoGDI is shown for reference.

engineering and replaced clusters of Lys, Glu or Gln with one of the five investigated amino acids.

The second issue was the optimization of the screening process, with the aim of enhancing the success rates of crystallization of the mutants without explicitly increasing the number of conditions used in the screens. To this end, we adopted the strategy of alternative reservoir solutions (Newman, 2005; Dunlop & Hazes, 2005). We present results that show how a combination of surface mutagenesis coupled with screening using the alternative reservoir approach can dramatically improve the crystallization success rates. While we confirm that alanines work extremely well to mediate crystal contacts, we show that tyrosines and threonines can also be used, particularly when solubility problems are encountered as a consequence of removing several charged surface residues by mutagenesis.

2. Materials and methods

2.1. Generation of mutants

The template for all mutants used in this study was the GST-fusion protein of the Δ66 N-terminal truncation of RhoGDI, which contains residues 67–204 of human RhoGDI with an rTEV protease-cleavage site between the tag and RhoGDI (Sheffield *et al.*, 1999). The QuikChange protocol (Stratagene, Inc.) was used for mutagenesis. In some cases, particularly with mutants that required long primers, a modified protocol that uses two-stage PCR was used (Wang & Malcolm, 1999). Primers were obtained from Operon Inc. Following mutagenesis, the plasmids were sequenced and transformed into the BL21(DE3) strain of *Escherichia coli* for expression. Expression and purification was performed as previously described (Longenecker, Garrard *et al.*, 2001). Briefly, the fusion protein was isolated using a glutathione Sepharose affinity column and cleaved with rTEV. The cleaved product was then passed through another glutathione Sepharose column to remove GST and uncut

Table 1

Composition of the custom screen used in this study (Page & Stevens, 2004; Page *et al.*, 2003; Kimber *et al.*, 2003).

	Organics	Salts	Buffer
1	50%(w/v) PEG 400	0.2 M lithium sulfate	0.1 M sodium acetate pH 4.5
2	20%(w/v) PEG 3000		0.1 M sodium citrate pH 5.5
3	20%(w/v) PEG 3350	0.2 M diammonium citrate	
4	30%(v/v) MPD	0.02 M calcium chloride	0.1 M sodium acetate pH 4.6
5	20%(w/v) PEG 3350	0.2 M magnesium formate	
6	20%(w/v) PEG 1000	0.2 M lithium sulfate	0.1 M sodium phosphate pH 4.2
7	20%(w/v) PEG 8000		0.1 M CHES pH 9.5
8	20%(w/v) PEG 3350	0.2 M ammonium formate	
9	20%(w/v) PEG 3350	0.2 M ammonium chloride	
10	20%(w/v) PEG 3350	0.2 M potassium formate	
11	50%(v/v) MPD	0.2 M ammonium phosphate	0.1 M Tris pH 8.5
12	20%(w/v) PEG 3350	0.2 M potassium nitrate	
13		0.8 M ammonium sulfate	0.1 M citric acid pH 4.0
14	20%(w/v) PEG 3350	0.2 M sodium thiocyanate	
15	20%(w/v) PEG 6000		0.1 M Bicine pH 9.0
16	10%(w/v) PEG 8000, 8%(v/v) ethylene glycol		0.1 M HEPES pH 7.5
17	40%(v/v) MPD, 5%(w/v) PEG 8000		0.1 M sodium cacodylate pH 6.5
18	40%(v/v) ethanol, 5%(w/v) PEG 1000		0.1 M sodium phosphate pH 4.2
19	8%(w/v) PEG 4000		0.1 M sodium acetate pH 4.6
20	10%(w/v) PEG 8000	0.2 M magnesium chloride	0.1 M Tris pH 7.0
21	20%(w/v) PEG 6000		0.1 M sodium citrate pH 5.0
22	50%(v/v) PEG 200	0.2 M magnesium chloride	0.1 M sodium cacodylate pH 6.5
23		1.6 M sodium citrate pH 6.5	
24	20%(w/v) PEG 3350	0.2 M tripotassium citrate	
25	30%(v/v) MPD	0.02 M calcium chloride	0.1 M sodium acetate pH 4.6
26	20%(w/v) PEG 8000	0.2 M sodium chloride	0.1 M sodium phosphate pH 4.2
27	20%(w/v) PEG 6000	1.0 M lithium chloride	0.1 M citric acid pH 4.0
28	20%(w/v) PEG 3350	0.2 M ammonium nitrate	
29	10%(w/v) PEG 6000		0.1 M HEPES pH 7.0
30		0.8 M sodium phosphate, 0.8 M potassium phosphate	0.1 M HEPES pH 7.5
31	40%(v/v) PEG 300		0.1 M sodium phosphate pH 4.2
32	10%(w/v) PEG 3000	0.2 M zinc acetate	0.1 M sodium acetate pH 4.5
33	20%(v/v) ethanol		0.1 M Tris pH 8.5
34	25%(v/v) 1,2-propanediol, 10%(v/v) glycerol		0.1 M Na/K phosphate pH 6.2
35	10%(w/v) PEG 20 000, 2% dioxane		0.1 M Bicine pH 9.0
36		2.0 M ammonium sulfate	0.1 M acetate pH 4.6
37	10%(w/v) PEG 1000, 10%(w/v) PEG 8000		
38	24%(w/v) PEG 1500, 20%(v/v) glycerol		
39	30%(v/v) PEG 400	0.2 M magnesium chloride	0.1 M HEPES pH 7.5
40	50%(v/v) PEG 200	0.2 M sodium chloride	0.1 M Na/K phosphate pH 6.2
41	30%(w/v) PEG 8000	0.2 M lithium sulfate	0.1 M sodium acetate pH 4.5
42	70%(v/v) MPD		0.1 M HEPES pH 7.5
43	20%(w/v) PEG 8000	0.2 M magnesium chloride	0.1 M Tris pH 8.5
44	40%(v/v) PEG 400	0.2 M lithium sulfate	0.1 M Tris pH 8.5
45	40%(v/v) MPD		0.1 M Tris pH 8.0
46	25.5%(w/v) PEG 4000, 15% glycerol	0.17 M (NH ₄) ₂ SO ₄	
47	40%(v/v) PEG 300	0.2 M calcium acetate	0.1 M sodium cacodylate pH 6.5
48	14%(v/v) 2-propanol, 30% glycerol	0.14 M calcium chloride	0.07 M sodium acetate pH 4.6
49	16%(w/v) PEG 8000, 20% glycerol	0.04 M potassium phosphate	
50		1.0 M sodium citrate	0.1 M cacodylate pH 6.5
51		2.0 M ammonium sulfate, 0.2 M sodium chloride	0.1 M cacodylate pH 6.5
52	10%(v/v) 2-propanol	0.2 M sodium chloride	0.1 M HEPES pH 7.5
53		1.26 M ammonium sulfate, 0.2 M lithium sulfate	0.1 M Tris pH 8.5
54	40%(v/v) MPD		0.1 M CAPS pH 10.5
55	20%(w/v) PEG 3000	0.2 M zinc acetate	0.1 M imidazole pH 8.0
56	10% 2-propanol	0.2 M zinc acetate	0.1 M sodium cacodylate pH 6.5

Table 1 (continued)

Organics	Salts	Buffer
57	1.0 M diammonium phosphate	0.1 M acetate pH 4.5
58	1.6 M magnesium sulfate	0.1 M MES pH 6.5
59	10%(w/v) PEG 6000	0.1 M Bicine pH 9.0
60	14.4%(w/v) PEG 8000, 20% glycerol	0.08 M sodium cacodylate pH 6.5
61	10%(w/v) PEG 8000	0.1 M imidazole pH 8.0
62	30% Jeffamine M-600	0.1 M MES pH 6.5
63		0.1 M citric acid pH 5.0
64	20%(v/v) MPD	0.1 M Tris pH 8.0
65	20% Jeffamine M-600	0.1 M HEPES pH 7.5
66	50%(v/v) ethylene glycol	0.1 M Tris pH 8.5
67	10%(v/v) MPD	0.1 M Bicine pH 9.0
68		0.1 M Tris pH 8.5
69	2.0 M ammonium sulfate	0.1 M sodium cacodylate pH 6.5
70	1.4 M sodium acetate	0.1 M sodium citrate pH 5.6
71	0.2 M ammonium acetate	0.1 M sodium acetate pH 4.6
72	0.2 M ammonium acetate	0.1 M sodium acetate pH 4.6
73	0.2 M calcium chloride	0.1 M HEPES pH 7.5
74	0.2 M ammonium sulfate	0.1 M sodium cacodylate pH 6.5
75	1.5 M lithium sulfate	0.1 M HEPES pH 7.5
76	0.2 M lithium sulfate	0.1 M Tris pH 8.5
77	0.2 M magnesium acetate	0.1 M sodium cacodylate pH 6.5
78	0.2 M ammonium sulfate	0.1 M sodium acetate pH 4.6
79	0.2 M magnesium acetate	0.1 M sodium cacodylate pH 6.5
80	0.2 M sodium acetate	0.1 M Tris pH 8.5
81	1.0 M sodium acetate	0.1 M imidazole pH 8.0
82	0.2 M sodium acetate	0.1 M sodium cacodylate pH 6.5
	0.8 M sodium phosphate, 0.8 M potassium phosphate	0.1 M HEPES pH 7.5
83	0.2 M ammonium sulfate	
84	0.2 M ammonium sulfate	
85	2.0 M ammonium sulfate	
86	4.0 M sodium formate	
87	2.0 M sodium formate	0.1 M sodium acetate pH 4.6
88	8%(w/v) PEG 8000	0.1 M Tris pH 8.5
89	1.4 M sodium citrate	0.1 M HEPES pH 7.5
90	2.0 M ammonium sulfate	0.1 M HEPES pH 7.5
91	2%(w/v) PEG 400	0.1 M sodium citrate pH 5.6
92	20%(v/v) 2-propanol, 20%(w/v) PEG 4000	
93	10%(v/v) 2-propanol, 20%(w/v) PEG 4000	0.1 M HEPES pH 7.5
94	20%(w/v) PEG 8000	
95	30%(w/v) PEG 1500	
96	0.2 M magnesium formate	
	0.2 M calcium acetate	0.1 M sodium cacodylate pH 6.5

protein. The resulting RhoGDI mutants were further purified by size-exclusion chromatography using a Superdex 75 column. All mutants were concentrated to 10–15 mg ml⁻¹ for crystallization.

Nine clusters located in fully solvent-exposed loops and containing two or three Lys and/or Glu/Gln residues were selected for mutation. They were (A) K99,Q100, (B) K105,E106, (C) K135,K138,K141, (D) K138,K141, (E) E154,E155, (F) E155,E157, (G) E163,E164, (H) K199,K200 and (I) K98,K99. The distribution of these mutations is represented in Fig. 1. Only double or triple mutants were used in this study because previous experiments in our laboratory have shown that mutating single residues is generally not as effective for SER crystallization as replacing multiple residues. In each cluster the high-entropy residues were systematically replaced with five amino acids: alanine, histidine, serine, threonine and tyrosine. After several mutants of the B cluster (K105,E106) exhibited a significantly lower solubility than the wild-type protein and other mutants, the B series of mutations

was discontinued. All of the other mutants generated in this study were at least as soluble as the wild-type protein.

Throughout this paper, specific cluster/residue combinations will be referred to by a two-letter designation. The first letter corresponds to the mutation cluster, as presented above and in Fig. 1. The second letter is the single-letter abbreviation of the amino-acid used. Thus, the CY mutant contains the mutations K135Y, K138Y and K141Y, whereas the IA mutant contains the mutations K98A and K99A.

2.2. Crystallization screening

Each mutant protein was subjected to two types of screen. The first, referred to as the ‘traditional’ or ‘standard’ screen, was a sitting-drop vapor-diffusion screen performed by mixing the concentrated protein in a 1:1 ratio with each reagent of a custom-made sparse-matrix screen. The reservoir of each well was filled with the same screen solution as that mixed with the protein. The conditions of the screen (Table 1) were derived from published data-mining experiments (Page & Stevens, 2004; Page *et al.*, 2003; Kimber *et al.*, 2003). The first 67 reagents of this screen are very close to those of the JCSG+ Suite (Qiagen Inc). The second screen, referred to here as the ‘salt’ screen, was identical to the traditional screen with the exception that the reservoir of each well was filled with

1.5 M sodium chloride instead of the crystallization reagent. Drops consisting of 1 µl protein and 1 µl screen solution were initially set up manually and suspended over 100 µl reservoirs in CompactClover Crystallization Plates, but after the acquisition of a Mosquito crystallization robot, drops of 200 nl + 200 nl equilibrated against 60 µl reservoirs were set up using Corning 3554 plates. All screens were performed at room temperature. Several plates were set up manually as well as with the robot, yielding virtually identical results. Crystallization plates were examined after approximately 1 d, 3 d, one week and two months. The drop was only considered to be a ‘hit’ if any well defined crystals, no matter how small, could be detected by microscopic examination.

2.3. Solution and refinement of structures

Data for the FA, EA, FH and AS mutants were collected at the Southeast Regional Collaborative Access Team (SER-CAT) 22-ID beamline at the Advanced Photon Source,

Argonne National Laboratory. Data for the DY, CT and CH mutants were collected at the SER-CAT 22-BM beamline. Data for the DY, CY and GY mutants were collected on an R-AXIS IV detector using a Nonius FR591 generator with a high-brilliance anode equipped with Osmic confocal mirrors. Data for the FS structure were collected with a Rigaku/MS Saturn92 using a Micromax-007 generator. In all cases data were collected at ~100 K. All data were processed and scaled using *HKL-2000* (Otwinowski & Minor, 1997). Molecular-replacement calculations were performed using *AMoRe* (Navaza, 1994) and *Phaser* (McCoy *et al.*, 2005). Structures were refined using a combination of *REFMAC5* (Murshudov *et al.*, 1997) from the *CCP4* suite (Collaborative Computational Project, Number 4, 1994) and *Coot* (Emsley & Cowtan, 2004). Final models were validated using *MOLPROBITY* (Lovell *et al.*, 2003).

3. Results and discussion

3.1. Standard screen results

In concert with previous results, wild-type Δ66 RhoGDI failed to crystallize in the traditional screen. In contrast, 32 of the 40 RhoGDI mutants in this study crystallized in this screen (Fig. 2). Tyrosine, alanine and threonine all proved to be effective residues for use in the SER strategy. Tyrosine performed best, yielding a total of 81 hits for the eight clusters, although this is largely owing to a single mutant (DY; see §2 for mutant nomenclature and description), which produced 42% of all hits. However, two other tyrosine mutants also

	Ala		His		Ser		Thr		Tyr		Totals								
	Standard	Salt	Standard	Salt	Standard	Salt	Standard	Salt	Standard	Salt	Unique	Unique							
A	1	0	1	2	2	3	1	18	19	5	15	17	8	13	17	17	14	48	31
C	2	9	9	2	2	4	1	2	3	3	14	16	5	5	6	13	12	32	26
D	1	1	1	4	7	11	0	0	0	0	1	1	34	35	48	39	39	44	37
E	6	0	6	1	0	1	2	0	2	5	4	8	0	2	2	14	8	6	6
F	11	10	16	3	0	3	3	3	6	1	0	1	0	0	0	18	11	13	10
G	0	4	4	5	8	11	1	6	7	2	2	4	14	12	20	22	17	32	18
H	12	15	20	2	1	3	1	1	2	0	1	1	17	3	20	32	30	21	18
I	4	5	8	2	4	5	3	6	7	16	28	38	3	3	6	28	24	46	35
	37	44	65	21	24	41	12	36	46	32	65	83	81	73	119				

Figure 2 Tabulated results. The mutant designation (A–I) is shown on the left. Coloring within the table is primarily for readability. The yellow shaded cells below the main table contain the totals for each target-residue series. The yellow cells to the right of the main table contain the totals for each mutation cluster. The ‘conditions’ column within each target-residue series is the number of different conditions that produced hits when both screens were performed. The term ‘Unique’ in the ‘Totals’ section is the number of different crystallization conditions producing hits for the mutation cluster. The standard and salt screens were performed as described in §2.

performed well, with the GY and HY mutants yielding 14 and 17 hits, respectively.

The alanine and threonine mutants were equally productive, producing 37 and 32 hits, respectively. The alanine series contained two mutants with large numbers of hits (FA and HA, with 11 and 12 hits, respectively), with only one mutant, GA, failing to crystallize at all. Interestingly, half of the crystals for the threonine series came from one mutant, IT, while two mutants failed to crystallize.

The overall results for the histidine and serine series were less encouraging, although both series produced crystals and in that sense outperformed the wild-type protein. The most notable result for the histidine series is that it was the only target residue examined that produced at least one hit for each mutation cluster and that several of the crystals it generated in the initial screen were large enough to screen for diffraction directly from the drop.

While differences between the five amino acids are easier to define, the differences between individual clusters are less clear. Although the D cluster had the highest number of hits, 87% of those hits were for the DY mutant alone. Indeed, for the five highest scoring mutation clusters (D, H, I, G and F) over half of each cluster’s total was accumulated by one particular mutant from that series. The column labeled ‘Unique’ under the ‘Totals’ in the table depicted in Fig. 2 represents the number of different crystallization conditions that led to crystals for that cluster. For most of the clusters, this is a significant percentage of the total number of hits for that series. This means that each of the five amino acids had a correlation to a specific subset of crystallization conditions. An exception to this is the F mutation cluster, where all of the crystals for FH, FS and FT were grown in conditions that also gave hits for FA. All four of these mutants crystallized in condition 73. Conditions 23 and 89 yielded hits for FA, FS and FH.

A histogram of the hits generated in the standard screen is presented in Fig. 3. An examination of the conditions that

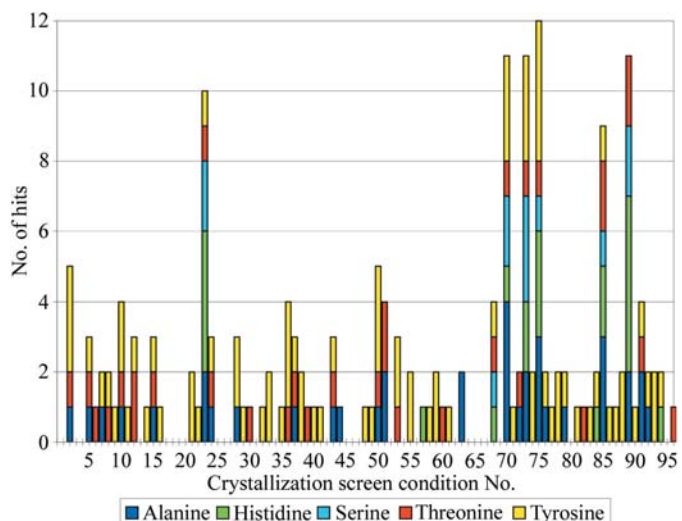


Figure 3 Histogram of hits in the standard screens.

Table 2
Crystal structures determined in this study.

	Crystallization condition	Cryo-additive	Reservoir†	$R_{\text{sym}}^{\ddagger}$ (%)	$R_{\text{work}}^{\ddagger}$ (%)	$R_{\text{free}}^{\ddagger}$ (%)	Resolution (Å)
AS§	18% (w/v) PEG 8000, 0.2 M calcium acetate, 0.1 M sodium cacodylate pH 6.5	Oil	1.5 M NaCl	8.5	26.3	33.4	2.8
CH (2jhs)	1.4 M sodium citrate, 0.1 M HEPES pH 7.5	10% glycerol	CS	4.2	17.8	20.8	1.95
CT (2jht)	35% PEG 4000, 0.2 M lithium sulfate, 0.1 M Tris pH 8.5	CR	1.5 M NaCl	13.2	22.2	25.9	1.88
CY (2bxw)	4.0 M sodium formate	CR	CS	9.0	17.8	22.1	2.4
DY1 (2ji0)	32% PEG 8000, 0.22 M ammonium sulfate, 0.1 M sodium cacodylate pH 6.5	35% PEG 8000	CS	4.0	18.4	25.8	2.1
DY2§	18% PEG 6000, 0.1 M Bicine pH 7.5	30% PEG 6000	CS	12.2	25.8	33.8	2.2
EA1 (2jhu)	2.0 M ammonium sulfate, 0.2 M sodium chloride, 0.1 M sodium cacodylate pH 6.5	10% glycerol	CS	7.2	20.9	23.2	1.65
EA2 (2jhv)	2.0 M ammonium sulfate, 0.2 M sodium chloride, 0.1 M sodium cacodylate pH 6.5	10% glycerol	CS	14.5	21.1	25.7	2.1
FA (2jhw)	2 M ammonium sulfate	15% glycerol	CS	5.1	22.0	26.1	2.5
FH1 (2jhx)	1.4 M sodium citrate, 0.1 M HEPES pH 7.5	10% glycerol	CS	6.8	19.4	21.9	1.6
FH2 (2jhy)	1.4 M sodium citrate, 0.1 M HEPES pH 7.5	10% glycerol	CS	6.5	22.4	25	1.9
FS (2jhz)	1.4 M sodium citrate, 0.1 M HEPES pH 7.5	10% glycerol	CS	9.3	18.6	22.7	2.2
GY§	30% PEG 4000, 0.2 M ammonium sulfate	CR	CS	8.1	30.0	43.7	2.5

† The reservoir was either the crystallization solution (CS) or 1.5 M sodium chloride. ‡ $R_{\text{sym}} = \sum_{\mathbf{h}} \sum_l |I_{\mathbf{h}l} - \langle I_{\mathbf{h}} \rangle| / \sum_{\mathbf{h}} \sum_l \langle I_{\mathbf{h}} \rangle$, where I_l is the l th observation of reflection \mathbf{h} and $\langle I_{\mathbf{h}} \rangle$ is the weighted average intensity for all observations l of reflection \mathbf{h} . R_{work} or $R_{\text{free}} = \sum_{hkl} ||F_{\text{obs}}(hkl)| - |F_{\text{calc}}(hkl)|| / \sum_{hkl} |F_{\text{obs}}(hkl)|$. § Owing to relatively poor data quality and because precise refinement of these structures was not critical for the conclusions of the study, these structures were not refined to a level justifying deposition in the Protein Data Bank.

produced crystals for each mutation cluster reveals that the conditions are a mixture of PEGs, alcohols and salts, in that order. Our custom crystallization screen has more conditions with polymers or organic solvents than salts as the precipitant;

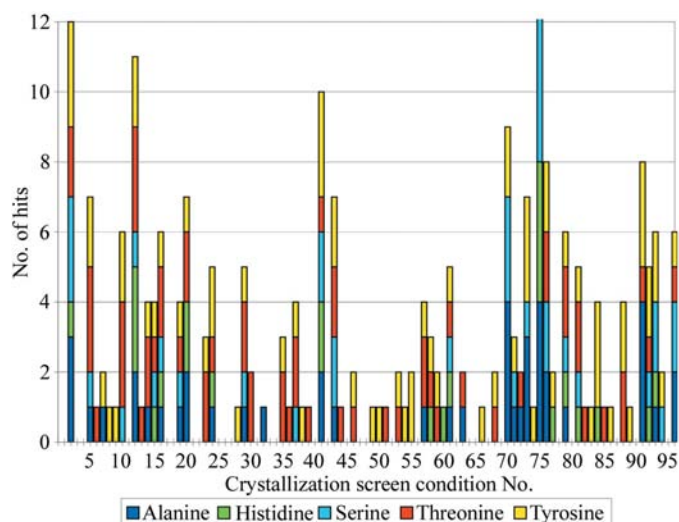


Figure 4
Histogram of hits in the salt screens.

thus, the intrinsic bias of the screen was reflected in the conditions that produced crystals, with the exception of the E mutation cluster. This cluster preferred salts as the precipitating agent.

3.2. Salt screen results

We selected 1.5 M NaCl as the alternative reservoir solution because of its previously reported performance in an unrelated study (Newman, 2005). Wild-type RhoGDI, which failed to crystallize in the traditional screen, produced crystals in one condition (No. 60) when 1.5 M NaCl was used as the reservoir solution.

Overall, the trends seen in the traditional screen were also evident in the salt screen (Fig. 2). The tyrosine series had the largest number of hits, with a large percentage (48%) accumulated by the DY mutant. Two other tyrosine mutants also produced high numbers of hits and only one (FY) failed to crystallize. Threonine and alanine were again second and third in terms of the number of hits. The threonine hits were primarily distributed among three of its mutants, but 43% of its hits were for the IT mutant. The histidine series

had the fewest hits in the salt screens, with two that did not have any. The serine mutants, which performed the poorest in the standard screen, performed better in the salt screen, generating 50% more hits than the histidine mutants. Two mutants did not crystallize at all.

For most of the clusters there was an apparent preference for a specific residue, although this bias was not quite as dramatic as with the standard screen. Five of the mutation clusters (D, E, F, H and I) had more than half of their hits scored by a single mutant. The cluster with the highest number of hits (A) had three mutants that scored high numbers of hits.

A histogram of the hits generated by the alternative reservoir screen is presented in Fig. 4. Unlike the broad range of conditions that yielded hits in the standard screen, it is primarily the polymer/organic precipitants that produce crystals. It is conceivable that the concentration of salt in the reservoir plays a role and that using a higher concentration, e.g. 2.0 M, may also increase the percentage of hits in the salt-based crystallization solutions.

3.3. Comparison of the standard and salt screens

Comparison of the standard and salt screens strongly supports the claim that using an alternative reservoir in

addition to the traditional screen can significantly increase the success rate of crystallization (Newman, 2005; Dunlop & Hazes, 2005). Overall, the salt screens produced almost 33% more hits than the traditional screens (242 compared with 183). For 27 of the 38 mutants that produced hits, the salt screen yielded as many or more hits than the standard screen, and in 18 of the 40 mutants it produced more hits.

An interesting outcome of the experiment was the increase in the number of conditions that yielded crystals. A quarter of the mutants examined in this study failed to produce any crystals in one of the screens, but produced at least one (and up to six) hits in the other screen. There was some overlap between crystallization conditions that gave hits in the two screens, but this was a relatively low percentage of the total number of hits for each mutant. The 'Conditions' columns in Fig. 2 within each target-residue series represent the number of different conditions that produced crystals for that mutant. Because the overlap between the conditions that give crystals in the two types of screens is limited, in many cases the number of conditions that yield an initial hit is greatly increased by performing both screens. Indeed, for the DY mutant 48 of the 96 conditions produced a crystal when both screens were performed. Even more important, however, is the fact that in those cases where there were low numbers of

hits in each of the screens, there was little overlap between the two.

Some of the differences between the two screens were easily detected by microscopic examination. For many conditions, there was a noticeable difference in the drop size when comparing equivalent drops in the standard and salt screens. Indeed, in some conditions the size of the drops actually increased in the salt screen, suggesting that the crystallization drop is actually being diluted owing to the higher concentration of salt in the crystallization solution than in the reservoir. Nonetheless, some of these conditions do produce crystals. More of the drops in the salt screen have a visible 'skin' after the plates have been equilibrated for several weeks.

Inexplicably, some mutants performed significantly better in one of the two screens. The AS mutant is a dramatic example of this, with 18 hits in the salt screen but only one hit in the standard screen. Conversely, the HY mutant produced 17 hits in the standard screen, but only three in the salt screen. In all, five mutants yielded high numbers of hits in one screen but not the other.

3.4. Cluster/target-residue correlations

While the results presented here clearly demonstrate that alanine, tyrosine and threonine are all potentially effective for



Figure 5

Crystals of the DY mutant showing the same basic morphology. The top four rows are from the standard screen and the bottom row is from the salt screen. The conditions that produced these crystals are (reading across and down) conditions 2, 10, 12, 15, 16, 29, 35, 36, 37, 49, 59, 61, 70, 71, 73, 75, 79, 88, 92 and 93 in the standard screen and conditions 5, 24, 73, 88 and 89 in the salt screen.

use in protein crystallization by SER, we also note that there appears to be a correlation between the type of amino acid and the structural context in which it is placed. In other words, certain mutation clusters yield high numbers of hits when a specific residue is introduced. For example, in the D mutation cluster, alanine, serine, threonine and histidine show modest efficacy. However, when tyrosines are used to replace the lysines in this cluster, the results are spectacular. The DY mutant yields a total of 69 hits in the two screens. Several other cluster/amino-acid combinations also stand out within their respective series. The IT mutant produced almost 50% more hits than all four of the other target residues for this cluster combined. Other examples include FA, CT, HA, HY and GY. We have no explanation at this point for this phenomenon.

We have also examined the crystallization conditions that produced the most hits for each type of amino acid, but we did not detect any trends consistent with a correlation between crystallization conditions and specific residues used for surface engineering.

3.5. Crystal forms and molecular packing

Although the 40 mutants screened in this study yielded hundreds of hits, microscopic inspection revealed a limited

spectrum of crystal morphologies, suggesting that the total number of crystal forms that are being generated might be relatively limited. For example, most of the DY mutant crystals showed similar morphologies (Fig. 5). We selected those crystals that were either large enough for direct analysis or that required relatively little effort to optimize, collected X-ray data, and solved the structures. The table in Fig. 6 shows a summary of the data along with characterization of crystal forms previously described by us (Longenecker, Garrard *et al.*, 2001; Mateja *et al.*, 2002; Czepas *et al.*, 2004) and Table 2 provides further details of the structures determined in the course of this study. We identified seven novel crystal forms, five monoclinic, one orthorhombic and one trigonal. We also found crystal forms that had been previously described: four mutants produced the same crystal form as the wild-type protein and two mutants produced a previously observed trigonal form. This larger than expected variety is of course a result of the fact that different packing modes can be accommodated within the same space-group symmetry and related space groups can show identical morphologies.

Overall, four crystal systems are represented by the 15 different crystal forms described so far for RhoGDI in this study and in previous papers. In a majority of cases, the crystal contacts are directly mediated by the mutated patches or the mutations are in the proximity of the contact. Also, 12 mutants

yielded unique crystal forms that were not observed for others. However, some crystal forms showed up repeatedly for different mutants. The *R32* form, identified originally for the wild-type and single-site K→A mutants (Longenecker, Garrard *et al.*, 2001), was also found for the EA, FH, FS and FA mutants (all of which involve closely spaced Glu154, Glu155 and Glu157). Remarkably, the FH mutant yielded crystals that diffracted to 1.6 Å, in stark contrast to the 2.4–2.8 Å resolution typically seen for the *R32* form. Another related trigonal form, *P3₂21*, was obtained for CA, CH and FH mutants. Thus, mutations of two different clusters, C and F, result in similar packing. The CY mutant also packs in a virtually identical fashion, except that the *c* axis is doubled and the dimer in the asymmetric unit now forms a *P3₁21* symmetry.

Just as different mutants can occasionally pack into the same crystal form, some mutants show a propensity to crystallize in several different forms. The FH mutant yields two different trigonal forms under identical crystallization conditions, while the DY mutant yields two monoclinic crystals under two different conditions. The

Structure	Protein	Space group	<i>a</i> (Å)	<i>b</i> (Å)	<i>c</i> (Å)	α (°)	β (°)	γ (°)	Resolution (Å)
Previously determined structures									
	WT-Del 66	<i>R32</i>	129.2	129.2	164.2	90	90	120	2.4
	WT-Del 66	<i>R32</i>	156.6	156.6	132.5	90	90	120	2.5
Ifst (CA+)	K135A,138A,141A,L196F	<i>R3</i>	125.2	125.2	82.7	90	90	120	2.0
I _{fso} (CA-long)	Δ 23 K135A,K138A,K141A	<i>P3₂21</i>	76.3	76.3	88.7	90	90	120	2.0
I _{f0}	K113A	<i>R32</i>	128.5	128.5	164.3	90	90	120	2.6
I _{f3}	K141A	<i>R32</i>	129.6	129.6	164.8	90	90	120	2.8
I _{kmt} (EA)	E154A,E155A	<i>P1</i>	34.1	35.9	67.5	79.2	82.7	76.4	1.25
I _{qvy}	K199R,K200R	<i>C2</i>	148.7	58.2	75.1	90	92.5	90	1.6
	E109A	<i>C2</i>	162.9	62.8	64.9	90	93.9	90	3.0
(EA + FA)	E154A, E155A, E157A	<i>R32</i>	130.4	130.4	163.7	90	90	120	2.8
(IR)	K98R, K99R	<i>P2₁2₁2</i>	79.5	111.8	37.9	90	90	90	2.3
(IR+)	K98R, K99R, K105R	<i>P2₁2₁2</i>	79.1	112.2	37.6	90	90	90	2.9
Structures determined as part of this study									
AS	K99A, Q100A	<i>P2₁2₁2</i>	86.2	110.1	76.1	90	90	90	2.8
CH	K135H, K138H, K141H	<i>P3₂21</i>	75.3	75.3	91.3	90	90	120	2.0
CT	K135T, K138T, K141T	<i>C2</i>	190.8	34	103.9	90	115.6	90	1.9
CY	K135Y,K138Y,K141Y	<i>P3₁21</i>	77.3	77.3	171.7	90	90	120	2.4
DY1	K138Y, K141Y	<i>P2₁</i>	32.0	55.1	38.9	90	107.5	90	2.1
DY2	K138Y, K141Y	<i>P2₁</i>	39.5	56.2	61.6	90	91.7	90	2.2
EA1	E154A,E155A	<i>R32</i>	129.6	129.6	166.6	90	90	120	2.8
EA2	E154A,E155A	<i>C2</i>	132.2	131.4	92.5	90	90.9	90	1.7
FA	E155A, E157A	<i>R32</i>	129.5	129.5	165.7	90	90	120	2.5
FH1	E155H, E157H	<i>R32</i>	130.1	130.1	162.9	90	90	120	1.6
FH2	E155H, E157H	<i>P3₂21</i>	75.2	75.2	91.6	90	90	120	1.9
FS	E155S, E157S	<i>R32</i>	130.6	130.6	163.4	90	90	120	2.2
GY	E163Y, E164Y	<i>P2₁</i>	43.3	157	43.2	90	92.7	90	2.5

Figure 6 RhoGDI crystal forms determined to date. The background shading in the leftmost columns indicate that the same mutant produced more than one structure. The background shading on the right indicates that the same crystal form was obtained with different mutants.

same is true of the EA mutants, which yield trigonal or monoclinic crystals depending on the conditions.

4. Conclusions and discussion

We have previously shown that replacing large highly entropic residues with alanines can facilitate crystallization (Longenecker, Garrard *et al.*, 2001; Mateja *et al.*, 2002), but we had not systematically examined the impact of residues other than alanine for generating crystal contacts. In this study, we addressed this question and we also looked at more efficient means of screening of the mutants in an effort to obtain X-ray quality crystals.

Our results show that residues other than alanine can effectively replace solvent-exposed lysines, glutamates and glutamines to generate more crystallizable protein variants. We specifically show that tyrosine and threonine work well to induce crystallization. Serine and histidine perform less well, yet still better than the wild-type RhoGDI. This is in general terms consistent with our expectations, based on the analysis of amino-acid occurrences at protein–protein interfaces (Conte *et al.*, 1999). Since lysines, glutamates and glutamines are all disfavored at interfaces (Bordner & Abagyan, 2005; Ofra & Rost, 2003) and their incorporation into crystal contacts is energetically prohibitive, it follows that almost any other amino acid should perform better in their place to induce crystallization. The question of which substituting residue would perform better than others is more difficult to answer. Alanines and threonines are not particularly favored at interfaces, but they are small and remove a major impediment to crystallization without necessarily creating ‘sticky’ patches. Tyrosines are known to play a key role at interfaces (Conte *et al.*, 1999; Fellouse *et al.*, 2004), particularly at antigen–antibody interfaces, and the dramatic enhancement of crystallizability of mutants containing tyrosines should not be a surprise. The poor performance of serine is unexpected because it is found in protein–protein interfaces with about the same frequency as threonine (Bordner & Abagyan, 2005; Conte *et al.*, 1999) and the histidines were only tested because they do occur at interfaces with higher frequency than others (Ofra & Rost, 2003) and have limited conformational flexibility.

Overall, the study strongly reaffirms the notion that replacement of high-entropy surface residues with amino acids that are more amenable to mediating intermolecular contacts is a powerful and effective approach for producing high-quality crystals for structural analysis. The question now is: what is the most efficient strategy that would result in a high, perhaps >90%, chance of obtaining crystals? We note that an average single-domain protein typically shows relatively few high-entropy clusters that are particularly suitable for the SER approach (Goldschmidt *et al.*, in preparation). We also observe that often a particular site will yield high-quality crystals in combination with one specific residue but not others. It follows that it may be more productive to prepare several different variants for one cluster, particularly those containing Ala, Tyr and Thr. At this time, we have not performed any mixed

substitutions where two residue types are used as replacement residues within one mutation cluster (*i.e.* K135A,K138Y, K138T). One could speculate that this type of substitution may be advantageous if a number of homologous proteins contain a particular sequence within the mutation cluster, but this remains to be tested.

It should be noted that while designing the mutants in this study we had the benefit of the knowledge of the structure of the protein we were trying to crystallize, which will not normally be the case for investigators resorting to surface entropy reduction, unless their objective is to obtain a novel crystal form with superior diffraction qualities. It is, however, possible to select mutation sites that have a high probability of solvent-exposure from amino-acid sequence alone and a significant number of previously undetermined structures has been solved using the SER technique. Three primary criteria need to be considered when selecting sites for mutagenesis: (i) the entropy of the residues within a continuous stretch, which can be represented as an entropy profile graphed by residue number, (ii) the predicted secondary structure and (iii) the sequence conservation. These three criteria, along with a number of other minor criteria, have been incorporated into a web-based server designed to suggest potential mutations. This SER prediction (SERp) server is freely available at <http://nihserver.mbi.ucla.edu/SER> and will be discussed elsewhere (Goldschmidt *et al.*, in preparation).

We also addressed the question of how to best screen the mutants. It appears that the alternative reservoir strategy works extremely well and offers a simple means of expanding the range of successful crystallization conditions. We note, however, that the improvement of the wild-type RhoGDI in the salt screen (one hit compared with no hits) was not as dramatic as some of the mutants examined in this study. This observation is again consistent with the premise that proteins intrinsically recalcitrant to crystallization cannot be easily crystallized by expanding the range of screens. In contrast, the engineered variants are very likely to benefit from this approach and yield numerous new crystal forms with altered packing and some with superior physical properties.

Screening with alternative reservoirs has several other advantages. One screen with an alternative reservoir requires only a microlitre or less of the crystallization solution. Even if both standard screen and alternative reservoir screens are performed for each protein, twice as many crystallization screens can be performed with the same volume of crystallization solutions, making this a very economical approach to screening. Another advantage is that it gives the crystallographer one more easy-to-optimize parameter once an initial hit has been found, *i.e.* the concentration of the alternate reservoir. It should also be noted that while we restricted our study to one alternate reservoir solution, recent publications regarding this screening procedure have examined several different alternative reservoir solutions, including ammonium sulfate and PEGs (Dunlop & Hazes, 2005; Newman, 2005).

The one disadvantage we have found with the alternative reservoirs is that it can be more difficult to find a suitable cryo-solution because the concentration of the components in the

equilibrated crystallization drop is unknown. In practice, sometimes these solutions are cryo-ready even if the original crystallization solution is not. When the equilibrated drop is not cryo-ready, using oil as a cryoprotectant has become one of our first approaches.

In the course of this crystallization experiment, 13 new structures of RhoGDI were determined. These particular mutants were selected for structure determination primarily based on the ease of crystallization-condition optimization and cryo-solution optimization. The PDB codes for the deposited structures are listed in Table 2.

The Integrated Center for Structure and Function Innovation is funded by NIH U54 GM074946. Use of the Advanced Photon Source was supported by the US Department of Energy, Office of Science, Office of Basic Energy Sciences under Contract No. W-31-109-Eng-38.

References

- Bielnicki, J., Devedjiev, Y., Derewenda, U., Dauter, Z., Joachimiak, A. & Derewenda, Z. S. (2006). *Proteins*, **62**, 144–151.
- Bordner, A. J. & Abagyan, R. (2005). *Proteins*, **60**, 353–366.
- Collaborative Computational Project, Number 4 (1994). *Acta Cryst.* **D50**, 760–763.
- Conte, L. L., Chothia, C. & Janin, J. (1999). *J. Mol. Biol.* **285**, 2177–2198.
- Czepas, J., Devedjiev, Y., Krowarsch, D., Derewenda, U., Otlewski, J. & Derewenda, Z. S. (2004). *Acta Cryst.* **D60**, 275–280.
- Dale, G. E., Oefner, C. & D'Arcy, A. (2003). *J. Struct. Biol.* **142**, 88–97.
- Devedjiev, Y., Surendranath, Y., Derewenda, U., Gabrys, A., Cooper, D. R., Zhang, R. G., Lezondra, L., Joachimiak, A. & Derewenda, Z. S. (2004). *J. Mol. Biol.* **343**, 395–406.
- Doye, J. P. K. (2004). *Phys. Biol.* **1**, 9–13.
- Dunlop, K. V. & Hazes, B. (2005). *Acta Cryst.* **D61**, 1041–1048.
- Emsley, P. & Cowtan, K. (2004). *Acta Cryst.* **D60**, 2126–2132.
- Fellouse, F. A., Wiesmann, C. & Sidhu, S. S. (2004). *Proc. Natl Acad. Sci. USA*, **101**, 12467–12472.
- Grueninger, D. & Schulz, G. E. (2006). *J. Mol. Biol.* **359**, 787–797.
- Hu, J. & Hubbard, S. R. (2006). *J. Mol. Biol.* **361**, 69–79.
- Janda, I., Devedjiev, Y., Cooper, D., Chruszcz, M., Derewenda, U., Gabrys, A., Minor, W., Joachimiak, A. & Derewenda, Z. S. (2004). *Acta Cryst.* **D60**, 1101–1107.
- Janda, I., Devedjiev, Y., Derewenda, U., Dauter, Z., Bielnicki, J., Cooper, D. R., Graf, P. C., Joachimiak, A., Jakob, U. & Derewenda, Z. S. (2004). *Structure*, **12**, 1901–1907.
- Kimber, M. S., Vallee, F., Houston, S., Necakov, A., Skarina, T., Evdokimova, E., Beasley, S., Christendat, D., Savchenko, A., Arrowsmith, C. H., Vedadi, M., Gerstein, M. & Edwards, A. M. (2003). *Proteins*, **51**, 562–568.
- Longenecker, K. L., Garrard, S. M., Sheffield, P. J. & Derewenda, Z. S. (2001). *Acta Cryst.* **D57**, 679–688.
- Longenecker, K. L., Lewis, M. E., Chikumi, H., Gutkind, J. S. & Derewenda, Z. S. (2001). *Structure*, **9**, 559–569.
- Lovell, S. C., Davis, I. W., Arendall, W. B. III, de Bakker, P. I., Word, J. M., Prisant, M. G., Richardson, J. S. & Richardson, D. C. (2003). *Proteins*, **50**, 437–450.
- McCoy, A. J., Grosse-Kunstleve, R. W., Storoni, L. C. & Read, R. J. (2005). *Acta Cryst.* **D61**, 458–464.
- Mateja, A., Devedjiev, Y., Krowarsch, D., Longenecker, K., Dauter, Z., Otlewski, J. & Derewenda, Z. S. (2002). *Acta Cryst.* **D58**, 1983–1991.
- Munshi, S., Hall, D. L., Kornienko, M., Darke, P. L. & Kuo, L. C. (2003). *Acta Cryst.* **D59**, 1725–1730.
- Murshudov, G. N., Vagin, A. A. & Dodson, E. J. (1997). *Acta Cryst.* **D53**, 240–255.
- Nadella, M., Bianchet, M. A., Gabelli, S. B., Barrila, J. & Amzel, L. M. (2005). *Proc. Natl Acad. Sci. USA*, **102**, 16830–16835.
- Navaza, J. (1994). *Acta Cryst.* **A50**, 157–163.
- Newman, J. (2005). *Acta Cryst.* **D61**, 490–493.
- Ofran, Y. & Rost, B. (2003). *J. Mol. Biol.* **325**, 377–387.
- Otwinowski, Z. & Minor, W. (1997). *Methods Enzymol.* **276**, 307–326.
- Page, R., Grzechnik, S. K., Canaves, J. M., Spraggon, G., Kreuzsch, A., Kuhn, P., Stevens, R. C. & Lesley, S. A. (2003). *Acta Cryst.* **D59**, 1028–1037.
- Page, R. & Stevens, R. C. (2004). *Methods*, **34**, 373–389.
- Prag, G., Misra, S., Jones, E. A., Ghirlando, R., Davies, B. A., Horazdovsky, B. F. & Hurley, J. H. (2003). *Cell*, **113**, 609–620.
- Sheffield, P., Garrard, S. & Derewenda, Z. (1999). *Protein Expr. Purif.* **15**, 34–39.
- Stevens, R. C. (2000). *Curr. Opin. Struct. Biol.* **10**, 558–563.
- Wang, W. & Malcolm, B. A. (1999). *Biotechniques*, **26**, 680–682.